

Thermal decomposition of AP/HTPB propellants in presence of Zn nanoalloys

Shalini Chaturvedi · Pragnesh N. Dave ·
Nikul N. Patel

Received: 4 December 2013 / Accepted: 27 January 2014 / Published online: 14 February 2014
© The Author(s) 2014. This article is published with open access at Springerlink.com

Abstract Composite solid propellants were prepared with and without nanoalloys (Zn–Cu, Zn–Ni, Zn–Fe), where nanoalloys are used as catalyst. Catalytic properties of these nanomaterials measured on ammonium perchlorate/hydroxyl-terminated polybutadiene propellant by thermogravimetric analysis and differential thermal analysis. Both experimental results show enhancement in the thermal decomposition of propellants in presence of nanoalloys. In differential thermal analysis method, experiments had done at three heating rates, $\beta_1 = 5^\circ$, $\beta_2 = 10^\circ$, $\beta_3 = 15^\circ$ per minute. Calculation of activation energy of high temperature decomposition step was done by using following Kissinger equation. Zn–Cu was found to be the best.

Keywords Propellants · Ammonium perchlorate · Burning rate · Activation energy · Thermal decomposition

Introduction

The nanomaterials show novel properties mainly due to their reduced dimensions, which result in domination of the surface over bulk (Alla et al. 2004; Liu et al. 2004; Peng et al. 2011; Wang et al. 2006). In the past two decades, the syntheses of metal nanoparticles received considerable attention due to their unusual properties and have optical, electrical, catalytic, magnetic potential applications, etc. In recent years, in area of synthesis of nanometal, several new processes are reported like polyol process (Pradhan et al.

2011) and microemulsion process (Chen and Hsich 2000). In material science, the range of properties of metallic system can be greatly extended by taking mixture of element to generate intermetallic compounds and alloys. The rich diversity of the compositions, structure and properties of metallic alloys has led to their widespread application in field of electronics and catalysis (Kurihara et al. 1995). Fabrication materials with well-defined, controllable properties and structure on the nanometer scale afforded by the intermetallic materials have generated interest in bimetallic nanoparticles (BMNs). Surface structure, composition and segregation properties of BMNs are of interest as they are important in the determining chemical activity, especially catalytic activity. Moreover, bimetallics are also of interest as they may display structures and properties which are distinct from those of the pure elemental cluster and bulk size bimetallics.

Solid propellants are mainly used in gun and rocket propulsion applications (Chaturvedi and Dave 2012a, b; Singh et al. 2009, 2011). They are very energetic and produce high temperature gaseous products on combustion. The high material density of solid propellants leads to high energy density (the energy produced by a unit volume of a propellant is called its energy density) needed for producing the required propulsive force. Propellants on board a rocket are burned in a controlled way (deflagration) to produce the desired thrust. Solid propellants are often tailored and classified by specific applications such as space launches, missiles, and guns. Different chemical ingredients and their proportions result in different physical and chemical properties, combustion characteristics, and performance (Beckstead et al. 2007).

Ammonium perchlorate (AP)-based composite propellants have been an important part in the field of solid rocket propulsion for more than five decades. This type of

S. Chaturvedi · P. N. Dave (✉) · N. N. Patel
Department of Chemistry, K.S.K.V. Kachchh University,
Mundra Road, Bhuj 370 001, Gujarat, India
e-mail: pragnesh7@yahoo.com

propellant typically contains a multi-modal distribution of AP (NH_4ClO_4) grains ($\sim 20\text{--}200$ μm) embedded in the hydroxyl-terminated polybutadiene (HTPB) matrix. The physiochemical processes that occur during the combustion of AP/HTPB propellant include condensed-phase heating, degradation of AP and HTPB, melting and surface pyrolysis, and gas-phase reactions. The flame structures and burning behavior depend on several factors, such as propellant composition, AP grain size, initial and ambient conditions, and propellant morphological configuration.

Several literatures reported earlier on the state of the knowledge up to the 1980s were written by Brill and Budenz (2000), Kishore (1979), and Ramohalli (1984). After lots of research efforts in the following years, AP-based propellants on account of the progress in experimental diagnostics and a numerical simulation are still the topic of interest.

In this article, we prepare composite solid propellants (CSPs). Bimetallic nanoalloys (BMNs) (Zn–Fe, Zn–Ni, Zn–Cu) are used as additives. Thermal decomposition of propellants was studied using TGA/DTA analysis. Activation energy was calculated by Kissinger equation, and the burning rate was also measured.

Experimental

AP (Qualigens) was used without further purification. Crystals of AP were ground into fine powder using a pestle and mortar and sieved to 100–200 mesh. NiCl_2 (Qualigens), ZnCl_2 (Analytical Rasayan), CuCl_2 (Merck), FeCl_2 (CDH Laboratory Reagent) Hydrazine (Merck) and Ethylene glycol (Merck) were used as received.

Preparation of BMNs

All BMNs were prepared as reported earlier by Wu and Chen 2003. An appropriate amount of metal chloride (2.5–45 mM) was dissolved directly in ethylene glycol followed by addition of an appropriate amount of hydrazine (0.05–0.9 M) and 1.0 M NaOH solution (10–72 μL). At 60 °C, metal nanoparticles were formed after 1 h in a capped bottle with stirring. The reaction was performed in an organic solvent instead of aqueous solution, so it was relatively easy to form pure metals. Nitrogen gas was produced and bubbled up continuously during the reaction which created an inert atmosphere and hence the passing extra N_2 gas was not necessary for the synthesis of pure BMNs.

Characterization of BMNs

Characterization of BMNs has done using powder XRD and SEM techniques (Figs. 1, 2). X-ray diffraction (XRD)

measurement was performed on the BMNs by an X-ray diffractometer using $\text{CuK}\alpha$ radiation ($\lambda = 1.5418$). The diffraction pattern is shown in Fig. 1. Particle size was calculated by applying Scherrer's equation (Birks and Friedman 1946) and values are reported in Table 1.

Preparation of CSPs

CSP samples were prepared by mixing (Krishna and Swami 1997) of AP [100–200 and 200–400 mesh (3:1)] with BMNs (1 % by wt.). The solid materials were mixed with HTPB in the ratio of 3:1. The binder part includes the curing agent (IPDI) in equivalent ratio to HTPB and plasticizer (DOA, 30 % to HTPB). During mixing of the solid components with HTPB, temperature was maintained at 60 °C for 1 h. The propellants were prepared with and without BMNs, casted into aluminum plates having dimensions 1 × 3 × 10 cm. The samples were cured in an incubator at 70 °C for 10–15 days (Singh and Prem 2003). An average of three measurements was taken which are within experimental error and results are reported in Table 2.

Measurement of burning rate

The cured propellant samples were cut into smaller pieces having dimensions 0.8 × 0.8 × 9.0 cm and burning rate was measured at ambient pressure by fuse wire (Singh and Prem 2003) technique. An average of three measurements was taken (See Table 2).

TGA/DTA Analysis of Propellants

The non-isothermal decomposition of propellants with and without BMNs was carried out in NETZSCH STA449F3 TG apparatus at a heating rate of 10 °C/min in N_2 atmosphere taking 20 mg of samples. The plots of TGA and DTA analyses are shown in Fig. 3 and Fig. 4, respectively.

In DTA method, experiments had done at three heating rates $\beta_1 = 5^\circ$, $\beta_2 = 10^\circ$, $\beta_3 = 15^\circ$ per minute. Independent to model free; calculation of activation energy of HTD step was done by using following Kissinger equation (Lu et al. 1991).

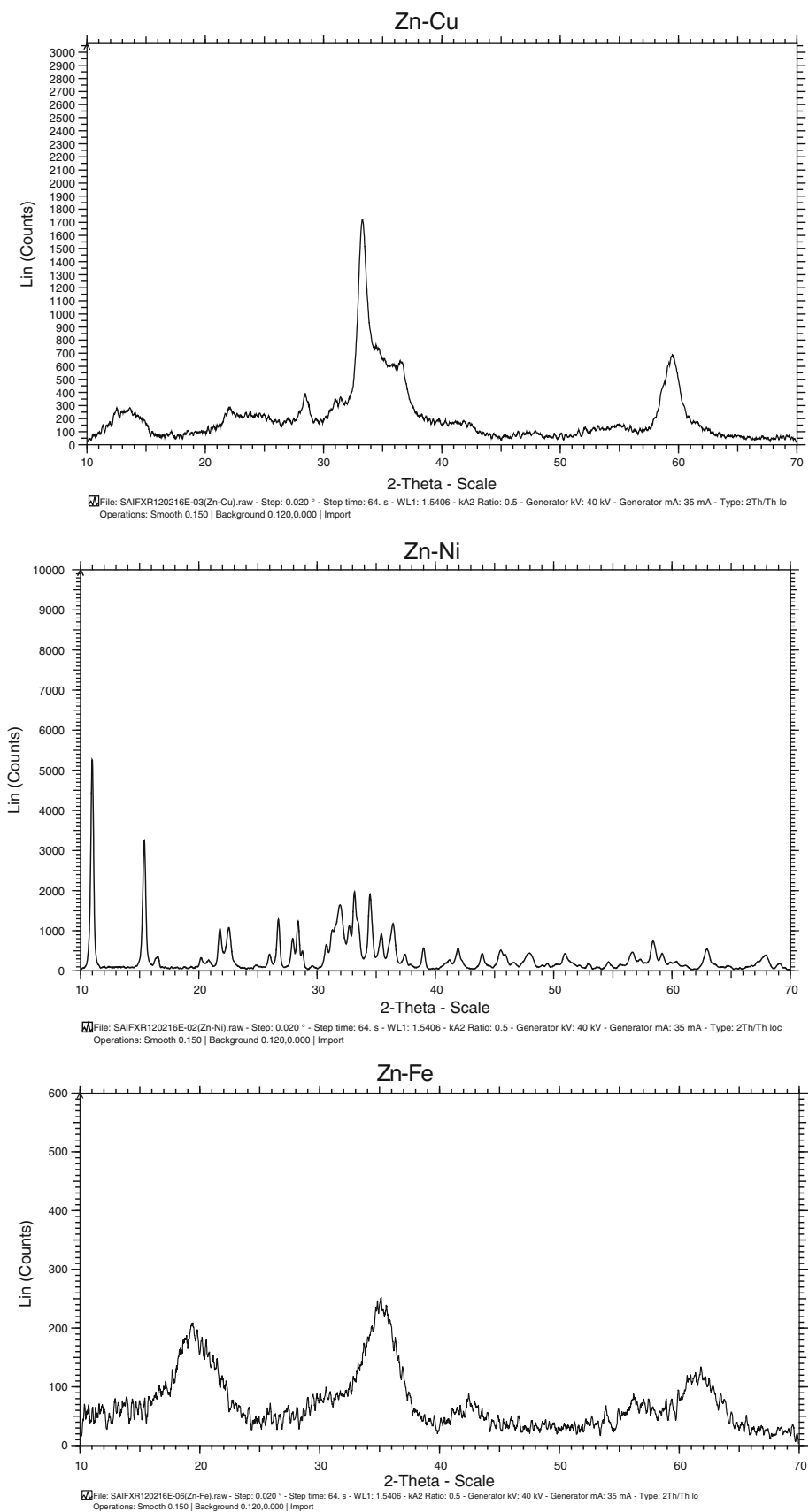
$$\frac{d\ln[\beta/T_{\max}^2]}{d[1/T_{\max}]} = \frac{(-E)}{R} \quad (1)$$

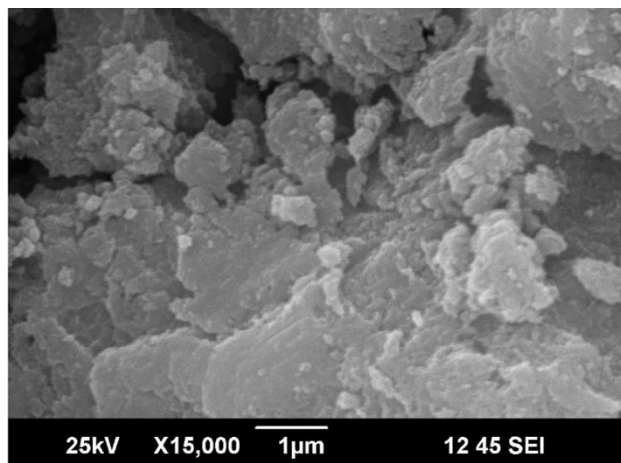
On differentiation

$$\ln[\beta/T_{\max}^2] = (-E)/RT + \text{Constant} \quad (2)$$

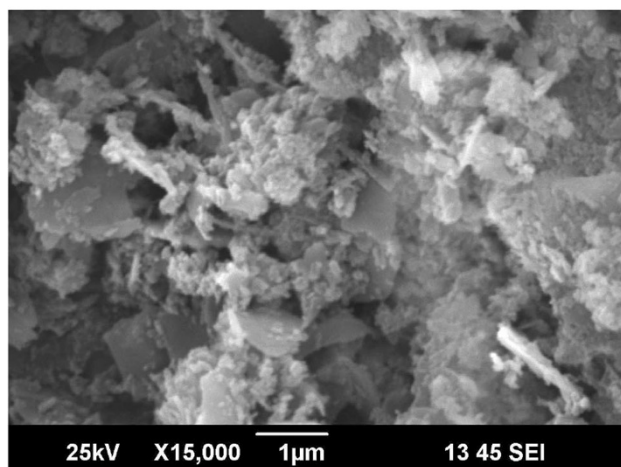
where β , E , R and T are the heating rate, activation energy, gas constant and specific temperature, respectively. A plot of $\ln(\beta/T^2)$ versus $1/T$ yields an approximate straight line with a slope of $-E/R$ (Fig. 5, Table 3).

Fig. 1 Powder XRD

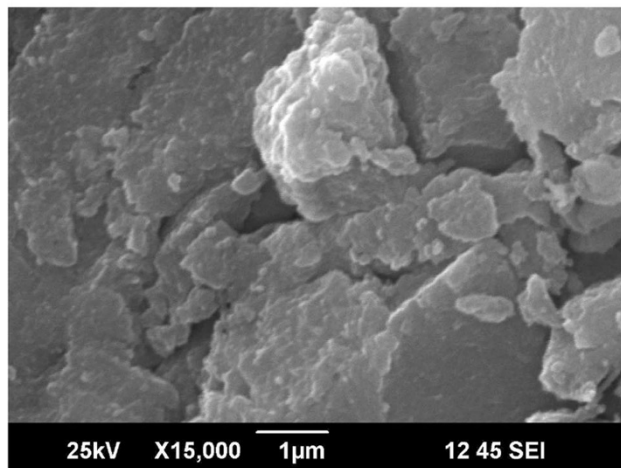




Zn-Cu



Zn-Ni



Zn-Fe

Fig. 2 SEM

Results and discussion

The XRD patterns (Fig. 1) for alloys Zn–Cu and Zn–Ni show considerable broadening of the peaks, which is due to

Table 1 Particle size of BMNs

| Nanoalloy | XRD Particle size (nm) |
|-----------|------------------------|
| Zn–Cu | 15.77 |
| Zn–Ni | 79.73 |
| Zn–Fe | 43.54 |

Table 2 DSC phenomenological data of the AP and AP with BMNs

| Samples | DSC | |
|------------|-----------------|--------|
| | Peak (Temp./°C) | Nature |
| AP | 285 | Exo |
| | 420 | Exo |
| AP + Zn–Cu | 278 | Exo |
| | 335 | Exo |
| AP + Zn–Ni | 279 | Exo |
| | 345 | Exo |
| AP + Zn–Fe | 280 | Exo |
| | 374 | Exo |

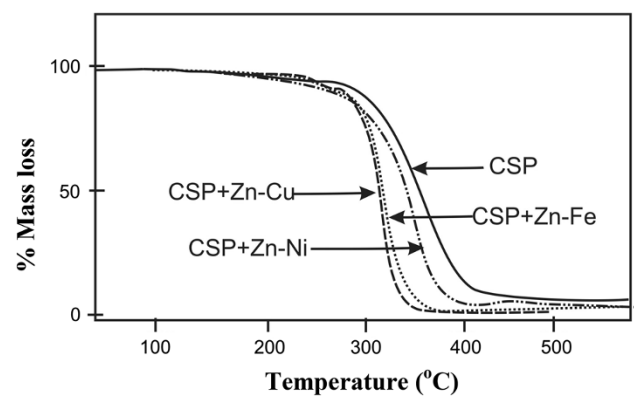


Fig. 3 TG thermogram

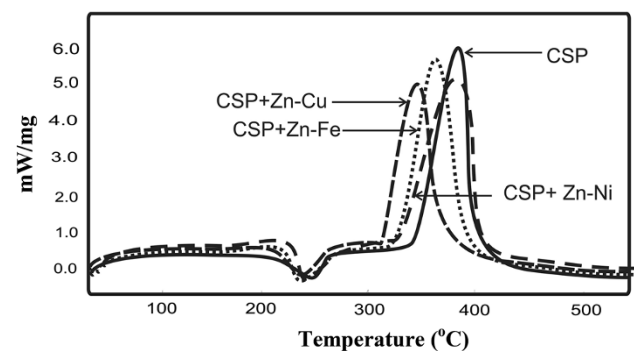


Fig. 4 DTA

the presence of very small particles. While no sharp peak observed in the XRD of Zn–Fe which indicates it is amorphous. Size of these very small particles (Table 1)

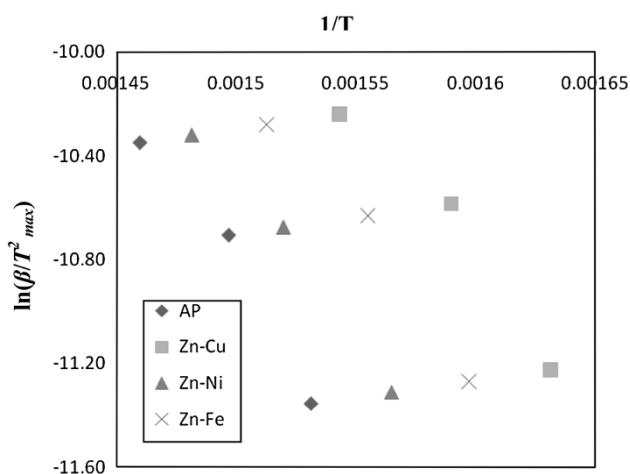


Fig. 5 Plot $\ln(\beta/T_{\max}^2)$ Vs $1/T$

Table 3 Burning rate of CSPs with and without BMNs (1 % by wt.)

| Sample | Burning rate (cm/sec) | r^*/r |
|-------------|-----------------------|---------|
| CSP | 4.891 | 1.00 |
| CSP + Zn–Cu | 4.040 | 1.32 |
| CSP + Zn–Ni | 4.270 | 1.15 |
| CSP + Zn–Fe | 4.118 | 1.47 |

r^* and r are burning rates of CSP with and without BMNs, respectively

shows beyond doubt that these prepared alloy are in the nanoscale range. SEM diagram of nanoalloys is shown in Fig. 2.

Most of the studies suggested that ballistic modifiers are active mainly in the condense phase at AP–binder interface (Chakravarthy et al. 1997). TG and DTA shown in Figs. 3 and 4 indicates that the condensed phase reactions are occurring in CSPs. CSPs have two-step decomposition namely LTD and HTD, whereas in case of propellants with BMNs, LTD almost disappears while HTD occurs at much lower temperature, which may be due to the activity of BMNs. Lowering of HTD was also supported by DTA.

The mass loss was accelerated when BMNs were used as catalysts (1 wt%) for CSPs. The mass loss might be enhanced on account of the acceleration of any decomposition of the HTPB, AP, and HTPB/AP. The result shows that the rate of polymer decomposition is enhanced when catalysts are added. Perhaps oxidative degradation of HTPB is increased by catalysts as it has been pointed out in earlier work (Singh et al. 2013).

In CSPs, AP particles first decompose in the sub-surface region to form perchloric acid (HClO_4), and the HTPB binder decomposes to produce fuel in the form of hydrocarbon fragments and hydrogen. HClO_4 decomposes further to form smaller oxidizing species. These decomposed gases consisting of fuel and oxidizer components mix

Table 4 Activation energy of HTD step

| Sample | Activation energy (E) (kJ/mol) |
|-------------|--------------------------------|
| CSP | 116.172 |
| CSP + Zn–Cu | 92.628 |
| CSP + Zn–Ni | 99.155 |
| CSP + Zn–Fe | 97.370 |

together to form a diffusion flame above the propellant-burning surface. The flame structure, however, is more complex as there are individual premixed monopropellant flames from AP and partially mixed flames from HTPB, in addition to the diffusion flame from their decomposition products. The luminous flame is attached to the burning surface and there is no dark zone as seen in double-base propellants (Ramakrishna et al. 2002; Summerfield 1984).

The combustion of AP/HTPB composite propellant involves an array of intricate physiochemical processes including: (1) conductive preheating, decomposition, and phase transition in the condensed phase; and (2) multi-stage reactions in the gas phase (Brewster and Mullen 2011).

The results reported in Table 3 clearly show that BMNs enhance the burning rate “ r ” of CSPs. Enhancement was best in presence of Zn–Cu alloys. It enhances the burning rate by 1.67 times.

Kinetics

The activation energy for LTD and HTD of CSPs under continuous heating was calculated by Kissinger equation. A plot of $\ln(\beta/T_{\max}^2)$ versus $1/T$ yields an approximate straight line with a slope of $-E/R$. Calculated activation energy of CSPs at HTD has been shown in the Table 4 which clearly shows the lowering in activation energy for HTD for CSP in presence of nanoalloys. Remarkable lowering has been found in presence of Zn–Cu alloys.

Summarizing these results, it may be inferred that BMNs can be used as catalyst for AP and CSPs while Zn–Cu was found to be the best.

Conclusion

Composite solid propellants were prepared with and without nanoalloys (Zn–Cu, Zn–Ni, Zn–Fe), where nanoalloys are used as catalyst. TGA analysis shows catalytic activity of CSPs of metal alloys was best as compared to metal alloys with AP. Burning rate study shows enhancement in burning rate with nanoalloys. Best results were found for Zn–Cu.

Acknowledgments The authors are grateful to Chemistry Department of KSKV University, Bhuj for laboratory facility. One of the

authors Shalini Chaturvedi is also thankful to CSIR for Research associate (RA) fellowship.

Open Access This article is distributed under the terms of the Creative Commons Attribution License which permits any use, distribution, and reproduction in any medium, provided the original author(s) and the source are credited.

References

- Alla P, Polina U, Yurii F, Sergey Z, Joop S (2004) Nanomaterials for heterogeneous combustion. *Propell Explo Pyrotech* 29(1):39–48
- Beckstead MW, Puduppakkam K, Thakre P, Yang V (2007) Modeling of combustion and ignition of solid-propellant ingredients. *Prog Energy Combust Sci* 6:497–551
- Birks LS, Friedman H (1946) Particle size determination from X-ray line broadening. *J Appl Phys* 17:687–692
- Brewster MQ, Mullen JC (2011) Burning-rate behavior in aluminized wide-distribution AP composite propellants. *Combust Explos Shock Waves* 47(2):200–208
- Brill TB, and Budenz BT (2000) Flash pyrolysis of ammonia perchlorate-hydroxylterminated-polybutadiene mixtures including selected additives. In: Yang V, Brill TB, Ren WZ, (eds.) Solid propellant chemistry, combustion and motor interior ballistics. *Prog Astronaut Aeronaut AIAA NY* 185: 3–23
- Chakravarthy SR, Price EW, Sigman RK (1997) Mechanism of burning rate enhancement of composite solid propellants by ferric oxide. *J Propuls Power* 13(4):471–480
- Chaturvedi S, Dave PN (2012a) Nano metal oxide: potential catalyst on thermal decomposition of ammonium perchlorate. *J Exp Nanosci* 7(2):205–231
- Chaturvedi S, Dave PN (2012b) A review on the use of nanometals as catalysts for the thermal decomposition of ammonium perchlorate. *J Saudi Chem Soc* 16(3):307–325
- Chen DH, Hsich C- H (2000) Synthesis of nickel nanoparticles in aqueous cationic surfactant solutions. *J Mater Chem* 12:2412–2415
- Kishore K (1979) Comprehensive view of the combustion models of composite solid propellants. *AIAA J* 171:216–224
- Krishna S, Swami RD (1997) Effect of catalyst mixing procedure on subatmospheric combustion characteristics of composite propellants. *J Propuls Power* 13(2):207–212
- Kuo KK, Summerfield M (eds) (1984) Fundamentals of solid propellant combustion, vol 90. AIAA, New York, p 891
- Kurihara LK, Chow GM, Schoen PE (1995) Nanocrystalline metallic powders and films produced by the polyol method. *Nanostrut Mate* 5:607–613
- Liu L, Li F, Tan L, Ming L, Yi Y (2004) Effects of nanometal Ni, Cu, Al and NiCu powders on the thermal decomposition of ammonium perchlorate. *Propell Explo Pyrotech* 29(1):34–38
- Lu K, Wei WD, Wang JT (1991) Grain growth kinetics and interfacial energies in nanocrystalline Ni-P alloys. *J Appl Phys* 69:7345–7347
- Peng Y-K, Lai C-W, Hsiao Y-H, Tang K-C, Chou P-T (2011) Multifunctional mesoporous silica-coated hollow manganese oxide nanoparticles for targeted optical imaging, T1 magnetic resonance imaging and photodynamic therapy. *Mater Express* 1:136–143
- Pradhan D, Mohapatra SK, Tymen S, Misra M, Leung KT (2011) Morphology-controlled ZnO nanomaterials for enhanced photoelectrochemical performance. *Mater Express* 1:59–67
- Ramakrishna PA, Paul PJ, Mukunda HS (2002) Sandwich propellant combustion: modeling and experimental comparison. *Proc Combust Instit* 29:2963–2973
- Ramohalli KNR (1984) Steady-state burning of composite propellants under zero cross flow situation. In: Kuo KK, Summerfield M (eds) Fundamentals of solid-propellant combustion; progress in astronautics and aeronautics. AIAA, New York
- Singh G, Prem Felix S (2003) Studies of energetic compounds, part 29: effect of NTO and its salts on the combustion and condensed phase thermolysis of composite solid propellants, HTPB-AP. *Combust Flame* 132:422–432
- Singh G, Kapoor IPS, Dubey S (2009) Bimetallic nanoalloys-preparation, characterization and catalytic activity. *J Alloy Compd* 480:270–274
- Singh G, Kapoor IPS, Dubey S (2011) Nanocobaltite: preparation, characterization and their catalytic activity. *Prop Explo Pyro* 36:367–372
- Singh G, Senguta SK, Kapoor IPS, Dubey S, Dubey R, Singh S (2013) Nanoparticles of transition metals as accelerants in the thermal decomposition of ammonium perchlorate. *J Ener Mat* 31(3):165–177
- Wang Y, Zhu J, Yang X, Lu L, Wang X (2006) Preparation of NiO nanoparticles and their catalytic activity in the thermal decomposition of ammonium perchlorate. *Thermochim Acta* 137:106–109
- Wu S-H, Chen D-H (2003) Synthesis and characterization of nickel nanoparticles by Hydrazine reduction in ethylene glycol. *J Colloid Interface Sci* 259:282–286